Geochemical Perspectives Letters

Zinc isotope evidence for volatile fluid remelting to form PGE-enriched reefs in layered intrusions

J.M.D. Day, F. Moynier

Supplementary Information

The Supplementary Information includes:

- Methods
- Supplementary Data Tables S-1, S-2
- Supplementary Figure S-1
- Supplementary Information References

Methods

Between 2.4 and 137 mg aliquots of powdered bulk rock or purified mineral separate were digested in a mixture of ultra-pure 4 parts HF and 1 part HNO_3 in Teflon beakers for 48 hours on a hotplate at 140 °C. Samples were dried down and treated with an Aqua Regia dissolution at the same temperature for 24 hours, dried down again and 6mol/L ultra-pure HCl was added to dissolve aliquots for another 24 hours at 140 °C on the hotplate.

Purification of Zn was achieved on particulate-free solutions using an improved anion-exchange chromatography method, with a recovery of 99.99 % (van Kooten and Moynier, 2019). Samples were loaded in 1.5 mol/L HBr on 0.1 ml AG1-X8 (200-400 mesh) ion-exchange columns with Zn being collected in 0.5 mol/L HNO_3. This step was repeated to purify Zn fractions. A procedural blank measured with samples was 0.2 ng, representing less than 0.1 % of total measured Zn for samples.

Isotopic compositions of Zn were measured with the *Thermo Fischer* Neptune Plus multi collector-inductively coupled plasma-mass spectrometer (MC-ICP-MS) housed at the Institut de Physique du Globe de Paris. Faraday cups were positioned to collect ions on masses 62, 63, 64, 65, 66, 67 and 68. Possible ^{64}Ni isobaric interferences were corrected by measuring the intensity of the ^{62}Ni peak. A solution containing 10 ppb Zn in 0.1 mol/L HNO_3 was prepared for isotopic analysis. Isotopic ratios of Zn in samples were analyzed using an Apex IR introduction system, combined with a 100 µl/min PFA nebulizer following Van Kooten and Moynier (2019). A single block of 30 ratios, in which the integration time of one scan was 8.3 seconds, was measured for each sample. Background was corrected by subtracting the on-peak zero intensities from a blank solution. The instrumental mass bias was corrected by bracketing each of the samples with standards and all data are reported relative to the JMC-Lyon standard solution. Standard reference materials BHVO-2 and AGV-2 gave δ^{66}Zn = +0.30 ± 0.04‰ (δ^{68}Zn = +0.64 ± 0.06 ‰; 100.2 µg/g Zn; n = 4) and δ^{66}Zn = +0.25 ± 0.08 ‰ (δ^{68}Zn = +0.53 ± 0.08 ‰; n = 6) respectively, consistent with recommended values (Moynier *et al.* 2017).

Supplementary Tables

Table S-1 Zinc isotope and abundance data for layered intrusion rocks.

Sample	Location	Rock Type	Mass (g)	µg/g	δ^{66}Zn	± 2σ	δ^{67}Zn	±2σ	δ^{68}Zn	± 2σ	n
Muskox Intrusion											
26A	Muskox	Chromitite	0.0463	270	0.16	0.04	0.25	0.10	0.35	0.11	4
4A	Muskox	Chromitite	0.0251	324	0.25	0.02	0.36	0.04	0.49	0.03	4
40A	Muskox	Chromitite	0.0361	295	0.31	0.03	0.42	0.03	0.60	0.01	4
CM19	Muskox-CMV	Glass Flow	0.1267	143	0.27	0.07	0.28	0.11	0.51	0.14	4
Stillwater Intrusion											
ST1203	Stillwater	Chromitite	0.0346	398	0.15	0.05	0.20	0.03	0.29	0.07	4
ST1204	Stillwater	Chromitite	0.0209	344	0.10	0.09	0.12	0.09	0.19	0.13	4
ST1217A	Stillwater	Chromitite	0.0683	146	0.14	0.07	0.19	0.09	0.27	0.12	4
JM Reef	Stillwater	Px pegmatoid	0.0154	69.0	0.22	0.03	0.35	0.03	0.43	0.02	4
JM Plagioclase	Stillwater	Mineral	0.0501	7.6	0.51	0.03	1.37	0.07	1.14	0.07	4
JM1 Pyrrhotite	Stillwater	Mineral	0.1370	1.8	0.02		0.16		0.07		1
JM2 Pyrrhotite	Stillwater	Mineral	0.0261	20.4	-0.03	0.06	0.03	0.11	-0.02	0.11	3
JM Pyrrhotite	Stillwater	Mineral	0.0533	2.8	ND		ND		ND		1
JM3 Chalcopyrite	Stillwater	Mineral	0.0889	352	0.68	0.04	0.98	0.07	1.35	0.08	4
JM Chalcopyrite	Stillwater	Mineral	0.0024	427	0.02	0.02	0.02	0.06	0.04	0.06	4
JM4 Pentlandite	Stillwater	Mineral	0.0802	27.3	0.44	0.14	0.72	0.18	0.98	0.24	4
JM Pentlandite	Stillwater	Mineral	0.0293	3.8	ND		ND		ND		1
JM Reef NM	Stillwater	Non-Magnetic	0.0344	61.8	0.17	0.08	0.23	0.13	0.34	0.15	4
JM Reef Mag	Stillwater	Magnetic	0.1179	106	0.29	0.02	0.40	0.10	0.55	0.06	4
Bushveld Intrusion											
BV18-14 Plagioclase	Bushveld	Mineral	0.1197	8	0.51	0.03	1.37	0.07	1.14	0.07	4
BV18-14 Phlogopite	Bushveld	Mineral	0.0959	49	0.45	0.04	0.66	0.05	0.87	0.06	4
BV18-14 Opx	Bushveld	Mineral	0.1213	75	0.45	0.01	0.66	0.03	0.87	0.03	4
BV18-14 Cpx 1	Bushveld	Mineral	0.1191	29	0.30	0.03	0.45	0.01	0.57	0.04	4
BV18-14 Cpx 2	Bushveld	Mineral	0.1240	13	0.08	0.07	0.11	0.08	0.14	0.12	4
BV18-14 E Spinel	Bushveld	Mineral	0.0149	991	-0.12	0.03	-0.19	0.05	-0.22	0.06	4
BV18-14 Big Spinel	Bushveld	Mineral	0.0229	713	-0.28	0.06	-0.43	0.08	-0.56	0.11	4
BV18-14 An Spinel	Bushveld	Mineral	0.0359	635	-0.30	0.03	-0.47	0.02	-0.60	0.05	4
BV18-14 Chalco 1	Bushveld	Mineral	0.0224	187	0.71	0.03	1.05	0.06	1.41	0.06	4
BV18-14 Chalco 2	Bushveld	Mineral	0.0145	218	0.61	0.03	0.91	0.06	1.21	0.09	4
BV18-14 Born	Bushveld	Mineral	0.0312	1.1	1.07		3.17		3.26		1
BV18-14 Pyrr	Bushveld	Mineral	0.0514	7.4	0.95		1.62		2.00		1
BV18-14 Pent	Bushveld	Mineral	0.0226	2.2	0.94		1.96		2.21		1
IRMM	Standard				0.28	0.04	0.48	0.06	0.60	0.09	4

Geochem. Persp. Let. (2025) 36, 13–17 | https://doi.org/10.7185/geochemlet.2527

Table S-2 Modal calculations for Zn isotopes in the JM and Merensky Reefs.

Sample	Sample Type	µg/g	δ^{66}Zn	Modal %	Modal 2 %
Stillwater Intrusion					
JM REEF		69.0	0.22		
Mag+NM Modes		***69.4***	***0.19***		
Mineral Modes		***67.6***	***0.22***		
	Non-Magnetic	61.8	0.17	0.83	
	Magnetitic	106	0.29	0.17	
	Plagioclase	7.6	0.51	0.30	
	Pyrrhotite	11.1	-0.01	0.50	
	Chalcopyrite	389	0.4	0.15	
	Pentlandite	27.3	0.44	0.05	
Bushveld Intrusion					
Merensky Reef		71	0.45		
Merensky Reef		***158***	***0.34***		
Merensky Reef 2		***81***	***0.40***		
BV18-14	Plagioclase	8	0.51	0.40	0.18
BV18-14	Phlogopite	49	0.45	0.01	0.01
BV18-14	Orthopyroxene	75	0.45	0.33	0.66
BV18-14	Clinopyroxene	21	0.19	0.02	0.03
BV18-14	Spinel	780	-0.23	0.16	0.04
BV18-14	Chalcopyrite	202	0.66	0.004	0.004
BV18-14	Bornite	1.1	1.07	0.005	0.005
BV18-14	Pyrrhotite	7.4	0.95	0.010	0.005
BV18-14	Pentlandite	2.2	0.94	0.006	0.004

Supplementary Figure

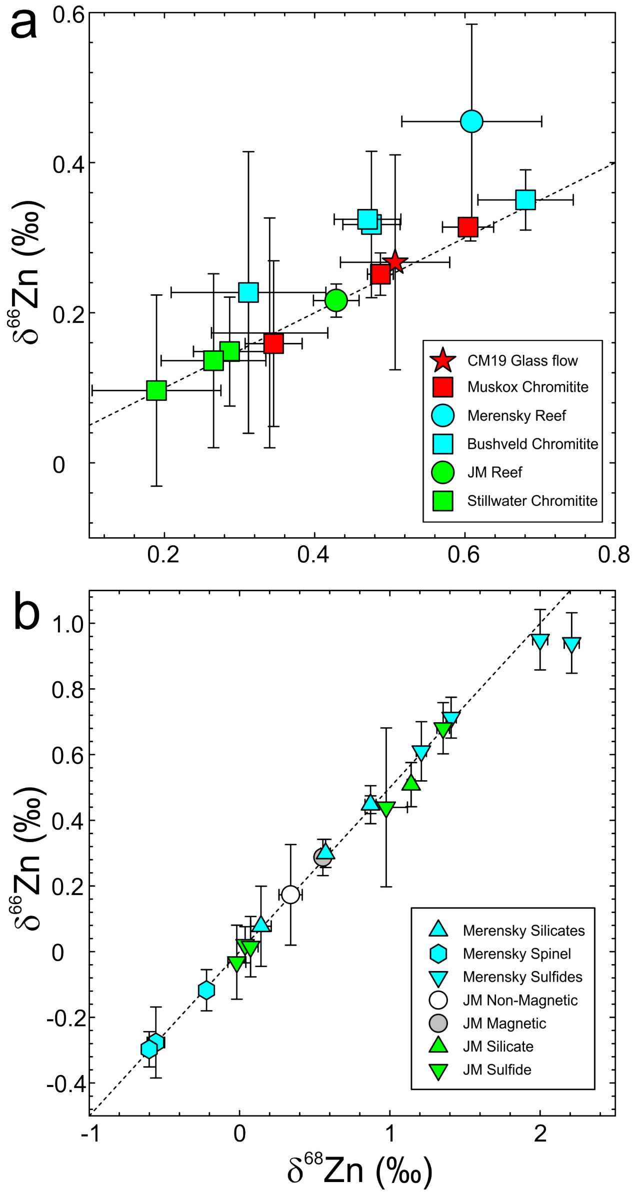

Figure S-1 Mass dependent behaviour of **(a)** bulk rock samples and **(b)** components of the Merensky and JM Reefs as a function of δ^{68}Zn versus δ^{66}Zn.

Supplementary Information References

Moynier, F., Vance, D., Fujii, T., Savage, P. (2017) The isotope geochemistry of zinc and copper. *Reviews in Mineralogy and Geochemistry* 82, 543-600. https://doi.org/10.2138/rmg.2017.82.13

van Kooten, E., Moynier, F. (2019) Zinc isotope analyses of singularly small samples (<5 ng Zn): Investigating chondrule-matrix complementarity in Leoville. *Geochimica et Cosmochimica Acta* 261, 248-268. https://doi.org/10.1016/j.gca.2019.07.022